Bioresource Technology xxx (xxxx) 130904

Contents lists available at ScienceDirect

Bioresource Technology

journal homepage: www.elsevier.com/locate/biortech

Enhanced biomass production and harvesting efficiency of *Chlamydomonas reinhardtii* under high-ammonium conditions by powdered oyster shell

Jikang Sui, Yuxuan Cui, Jinku Zhang, Shiyang Li, Yue Zhao, Mingkai Bai, Guangxin Feng *, Haohao Wu *

State Key Laboratory of Marine Food Processing & Safety Control, College of Food Science and Engineering, Ocean University of China, 5 Yushan Road, Qingdao, Shandong Province 266003, China

ARTICLE INFO

Keywords:
Medium acidification
Size-dependently
Liming agent
Supplement carbon source
Bio-flocculant

ABSTRACT

Chlamydomonas reinhardtii prefers ammonium (NH_4^+) as a nitrogen source, but its late-stage growth under high-NH_4^+ concentrations (0.5 ~ 1 g/L) is retarded due to medium acidification. In this study, oyster shell powders were shown to increase the tolerance of *C. reinhardtii* to NH_4^+ supplementation at 0.7 g/L in TAP medium in 1-L bubble-column bioreactors, resulting in a 22.9 % increase in biomass production, 62.1 % rise in unsaturated fatty acid accumulation, and 19.2 % improvement in harvesting efficiency. Powdered oyster shell mitigated medium acidification (pH 7.2–7.8) and provided dissolved inorganic carbon up to 8.02×10^3 μmol/L, facilitating a 76.3 % NH_4^+ consumption, release of up to 189 mg/L of Ca^{2+}, a 42.1 % reduction in ζ-potential and 27.7 % increase in flocculation activity of microalgae cells. This study highlights a promising approach to utilize powdered oyster shell as a liming agent, supplement carbon source, and bio-flocculant for enhancing biomass production and microalgae harvesting in NH_4^+-rich environments.

1. Introduction

Elevated levels of ammonium (NH_4^+) in various wastewater streams originating from both municipal and industrial sources pose significant environmental hazards. Conventional physical and chemical methods used for NH_4^+ removal encounter challenges such as high costs and energy consumption (Ye et al., 2018). NH_4^+ serves as the primary nitrogen source for the majority of microalgae due to its reduced energy demand for nitrogen assimilation. Utilizing microalgae for the effective transformation of NH_4^+ into valuable biomass has emerged as a feasible and environmentally friendly alternative to the traditional NH_4^+ removal methods. Notably, Chlorophytes exhibited a much higher tolerance to high levels of NH_4^+ (39000 μM) than diatoms, prymnesiophytes, etc. (Collos & Harrison, 2014). The release of at least one H^+ per NH_4^+ ion during assimilation and the late-stage growth of microalgae under high-NH_4^+ conditions is often hindered by the significantly reduced pH of the culture medium (Markou & Muylaert, 2016). To address this challenge, it is crucial to choose effective and cost-effective pH-buffering agents to improve microalgal biomass yield in high-NH_4^+ media.

Calcium carbonate ($CaCO_3$) is known for its size-dependent and slow-release pH-buffering capacity in soil and pond liming applications to improve fertility and oxygen levels (Morris et al., 2019). Oyster shells, predominantly composed of $CaCO_3$, are a viable and sustainable alternative source of calcium carbonate for agricultural liming practices (Bai et al., 2003; Surendra et al., 2022). $CaCO_3$ undergoes hydrolysis to generate CO_2, carbonate ions (CO_3^{2-}), and bicarbonate ions (HCO_3^-) under acidic conditions. The dissolved inorganic carbon (DIC) system can be represented by the following chemical equilibrium: $CO_2 + H_2O \leftrightarrow H_2CO_3 \leftrightarrow HCO_3^- + H^+ \leftrightarrow CO_3^{2-} + 2H^+$. Algae utilize two main mechanisms for CO_2 acquisition in cellular carbon fixation: (1) active uptake of HCO_3^- and/or CO_2, and (2) diffusive uptake of CO_2 (Giordano et al., 2005). HCO_3^- can be actively transported across cellular membranes through anion exchangers and/or converted to CO_2 by carbonic anhydrase in the periplasmic space, which is then absorbed and utilized by microalgal cells (Hurd et al., 2009; Mondal et al., 2017; Shitanaka et al., 2024). Each of these mechanisms is energy-dependent and collectively referred to as a carbon (or CO_2) concentrating mechanism (CCM). CCM has the potential to elevate the CO_2 concentration surrounding RuBisCO, which results in a significant improvement in the CO_2/O_2 ratio and a consequent increase in the rate of carbon fixation to promote cell growth (Su, 2021). Moreover, the hydrolysis of $CaCO_3$ yields Ca^{2+}, making it a safe and effective flocculant for enhancing microalgae harvesting (Pandey et al., 2019). Therefore,

* Corresponding authors.
E-mail addresses: fgx@ouc.edu.cn (G. Feng), wuhaohao@ouc.edu.cn (H. Wu).

https://doi.org/10.1016/j.biortech.2024.130904
Received 7 April 2024; Received in revised form 23 May 2024; Accepted 24 May 2024
0960-8524/© 20XX

oyster shells are a promising supplement for ameliorating medium pH and enhancing microalgal biomass production under high NH_4^+ conditions.

C. reinhardtii has a high-affinity NH_4^+ transport system that includes a surprisingly large set of NH_4^+ transporters (Ermilova EV, 2010) and is recognized for its efficient CO_2 fixation mechanism (Fukuzawa et al., 2001). Regulatory approvals for food applications in the United States and China further bolster their potential. Consequently, *C. reinhardtii* is a great candidate for the environmentally sustainable and economically feasible production of high-value biomolecules, particularly in NH_4^+-rich media (Darwish et al., 2020).

This study investigated the tolerance of *C. reinhardtii* to NH_4^+ and evaluated the effectiveness of powdered oyster shell as a medium supplement for enhancing biomass production from *C. reinhardtii* under high NH_4^+ conditions, followed by characterization of acid reduction and carbon source supplementation as the fundamental mechanisms involved. The role of Ca^{2+} from powdered oyster shell as a bio-flocculant to facilitate the harvesting of *C. reinhardtii* biomass under high NH_4^+ conditions was assessed. This study appears to be the first of its kind to assess the feasibility of using powdered oyster shell to improve both biomass production and harvesting efficiency of *C. reinhardtii* in high NH_4^+ scenarios.

2. Materials and methods

2.1. Microalgae strains and pre-culture

C. reinhardtii (FACHB-2217) was obtained from the Freshwater Algae Culture Collection at the Institute of Hydrobiology, Chinese Academy of Sciences (Wuhan, China). Before the experiment, microalgae were pre-cultured in a 250 mL Erlenmeyer flask containing 100 mL sterile Tris-acetate-phosphate (TAP) medium (Gorman & Levine, 1965) at 23 ± 1 °C under an illumination intensity of 30 μmol $m^{-2}s^{-1}$, and the flask was shaken manually twice a day (Banerjee et al., 2021).

2.2. Powdered oyster shell preparation

Oyster (*Crassostrea gigas*) shells were purchased from Qingdao Face-to-face Food Co., LTD (Shandong, China). They were washed with distilled water and immersed in 6 % NaOH solution for 6 h to remove surface-bound organic impurities. Subsequently, the samples were washed twice with distilled water and dried at 60 °C for 6 h before mechanical crushing (Liu et al., 2010). A muffle furnace was employed to incinerate oyster shells at 500 °C for 6 h, and the resulting ash was collected for the determination of $CaCO_3$ content (SX2-2.5–12 N, Yiheng, China). The powdered oyster shell was subjected to nitric-perchloric acid digestion to determine trace elements using inductively coupled plasma mass spectrometry (ICP-MS) with an Agilent 8800 triple quadrupole instrument (8800, Agilent, USA). For particle size sorting, the powder was successively filtered through meshes with sizes of < 0.15, 0.15 ~ 0.6, 0.6 ~ 1, and 1 ~ 2 mm.

2.3. Preparation of high-density microalgae seeds

C. reinhardtii were cultivated photoautotrophically in a 250 mL flask with 150 mL TAP medium until the middle logarithmic growth phase and harvested via centrifugation at 3 000 × g for 5 min. To prepare high-density seeds, cell pellets were transferred to 600 mL sterilized TAP medium supplemented with 1 g L^{-1} sodium acetate in an 800 mL column for mixotrophic cultivation (Moon et al., 2013). To facilitate carbon supply and culture mixing, compressed air with 0.04 % CO_2 (40 mL min^{-1}) was introduced by a 0.45 μm millipore filter membrane at the top of the column to avoid bacterial contamination. The culture was maintained under continuous white fluorescence light (40 ± 10 μmol $m^{-2}s^{-1}$) and at a constant temperature of 25 °C in a thermostatic incubator, and high-density algae seeds (~0.8 g L^{-1}) were successfully obtained within 4 d (see Supplementary Fig. 1). All the trials were repeated at least three times.

2.4. NH_4^+ tolerance assay

The full-strength TAP medium used for the control group, whereas N-deficient TAP medium supplied with high concentration NH_4Cl (0.5, 0.7, 1.0, and 1.5 g/L NH_4^+) as experimental groups, were correspondingly abbreviated as TAP, TAP + 0.5NH_4^+, TAP + 0.7NH_4^+, TAP + 1.0NH_4^+, and TAP + 1.5NH_4^+, respectively. To assess their NH_4^+ tolerance, *C. reinhardtii* was inoculated in 600 mL of medium with different NH_4^+ contents at 0.8 g/L biomass and cultivated in 1 L cylindrical bubble column bioreactors of 5 d. Compressed air with 0.04 % CO_2 (60 mL min^{-1}) was introduced into a 0.45 μm millipore filter membrane at the top of the column to avoid bacterial contamination. The culture was maintained under continuous white fluorescent light (80 ± 10 μmol $m^{-2}s^{-1}$) at a constant temperature of 25 °C in a thermostatic incubator. The levels of OD750, NH_4^+, and pH were recorded every day during the following 4 d of cultivation. Two sets of experiments were conducted to evaluate the effects of solution pH and NH_4^+ concentration on microalgae growth. In one experiment, the experimental trial medium pH was adjusted to 6.5, 6.0, and 5.5 respectively with 1 N HCl throughout the 5 d of cultivation using an automatic acid-base titrator (ZDJ-4B, Leici, China), and the control group was TAP medium (pH = 7). *C. reinhardtii* were seeded in 600 mL TAP medium with different pH at 0.8 g/L biomass and cultivated in 1 L cylindrical bubble column bioreactors for 5 d, the level of OD750 was monitored every day. In another experiment, the pH of the medium for groups was adjusted to ~ 7 by adding 1 N NaOH or HCl during the cultivation, repeated these five experiments (TAP, TAP + 0.5NH_4^+, TAP + 0.7NH_4^+, TAP + 1.0NH_4^+, and TAP + 1.5NH_4^+), and the levels of OD750 and NH_4^+ were recorded every day.

2.5. Supplementation of oyster shell powders for high-NH_4^+ microalgae cultivation

C. reinhardtii were seeded in 600 mL TAP + 0.7NH_4^+ medium at 0.8 g/L biomass and cultivated in 1 L cylindrical bubble column bioreactors for 96 h. Compressed air with 0.04 % CO_2 (60 mL min^{-1}) was introduced into a 0.45 μm millipore filter membrane at the top of the column to avoid bacterial contamination. The culture was maintained under continuous white fluorescence light (80 ± 10 μmol $m^{-2}s^{-1}$) and at a constant temperature of 25 °C in a thermostatic incubator. Two sets of experiments were conducted to evaluate the effects of powdered oyster shell supplementation on microalgae growth. In the first experiment, to evidence the liming action of powdered oyster shell, the medium pH dropped below 5.6 after 12 h, and then oyster shell powders with sizes of < 0.15 mm, 0.15 ~ 0.6 mm, 0.6 ~ 1 mm, and 1 ~ 2 mm were introduced into the medium at a dose of 1 g/L. In the second experiment, oyster shell powders (<0.15 mm) were incorporated at a dose of 1 g/L into the medium at the start of the experiment as the experimental group, and the medium pH was maintained at 7.5 with 1 N NaOH throughout the 96 h of cultivation using an automatic acid-base titrator as the control group (ZDJ-4B, Leici, China). Biomass, pH, NH_4^+, Ca^{2+}, dissolved inorganic carbon (DIC), and relevant gene transcription levels were recorded (6, 12, and 15 h) during cultivation. Cell pellets were obtained via centrifugation (3 000 × g, 5 min) for biochemical analysis. The concentrations of NH_4^+ in 0.22 μm filtrates of the culture media were determined spectrophotometrically by using Nessler's reagent method (Zhao et al., 2019). The concentrations of Ca^{2+} in 0.22 μm filtrates of the culture media were quantitated using an atomic absorption spectrophotometer (AA-6800, Shimadzu, Japan). DIC was measured on 40 mL filtered (0.45 μm pore size filters) medium samples using a Skalar Formacs$^{HT/TN}$ TOC/TN analyzer and

Skalar LAS-160 autosampler (AS-C5; Apollo SciTech Inc., USA). DIC was quantified using peak area correlation against a standard curve from a bicarbonate-carbonate mixture (Zhang & Hu, 2023).

2.6. Settling efficiency and zeta potential determination

At the end of the experiment, the zeta potential of microalgae cells in culture suspension was measured on a Zetasizer Nano ZS instrument (Malvern, Germany), and then culture suspension was left to sediment for 3 h, followed by the OD750 measurement of top supernatant. Settling efficiency was calculated as follows: settling efficiency (%) = (A – B)/A × 100, where A and B are the OD750 values of culture suspension and top supernatant, respectively.

2.7. Flocculation experiment

The effect of Ca^{2+} on the flocculation efficiency was determined using a jar test, and different concentrations (0, 40, 80, 120, 200, 400, 600, 800, and 1000 mg L^{-1}) of calcium ion solutions were prepared using calcium chloride. Algal suspensions with biomass concentrations of 0.1, 1.0, and 2.0 g/L were obtained through dilution. The algal suspension (100 mL) was stirred at 250 rpm in a 100 mL beaker. After the flocculant was added, stirring continued for 2 min. The stirring was stopped, and the suspension was allowed to set for 3 h when an aliquot of the supernatant was taken 2 cm from the surface of the liquid, and its absorbance at 550 nm was measured in a 10-mm path length plastic cuvette using a UV-2550 spectrophotometer (UV-2550, Shimadzu, Japan). Flocculation efficiency was calculated as follows: flocculation efficiency (%) = (Calgae – Calgae in the supernatant)/ Calgae × 100. Calgae in the supernatant is the concentration of algae still in the supernatant, and Calgae is the concentration of algae before the addition of flocculant.

2.8. Determination of microalgae growth and biomass production

Microalgae growth was determined by measuring the optical density at 750 nm (OD750) in 1-cm glass cuvettes on a UV-2550 spectrophotometer (UV-2550, Shimadzu, Japan). Biomass production was determined gravimetrically by measuring dry cell weight. In the experimental group with powdered oyster shell, aeration was halted initially, extract 10 mL of the solution after a 2-minute settling period. The dry weight of the microalgae cells was measured by filtering an aliquot of the culture suspension through a pre-weighed Whatman filter paper (GF/C). The filter paper was rinsed twice with distilled water and dried at 105 °C until it reached a constant weight. Biomass productivity was expressed in grams per unit volume per day (g $L^{-1}d^{-1}$). A linear regression equation was developed between OD750 and microalgae dry cell weight (g L^{-1}).

2.9. Biochemical analysis of microalgae biomass

The contents of water-soluble polysaccharides (WSP) and total carbohydrates in *C. reinhardtii* biomass were determined by the phenol–sulfuric acid method as described in the previous work (He et al., 2016). The soluble protein (SP) content in *the C. reinhardtii* biomass was analyzed using a BCA Assay Kit (PC0020, Solarbio, China). The lipid content in *the C. reinhardtii* biomass was measured using the chloroform–methanol method, stated by Trivedi et al. as previously described. (Trivedi et al., 2022). For fatty acid profiling, lipids were converted to fatty acid methyl esters by incubation in sulfuric acid/methanol (1:50, w/v) at 85 °C for 2.5 h with nonadecanoic acid (C19:0) as an internal standard, and then gas chromatography analysis was performed on a Varian 450-GC (Varian Inc., USA) with nitrogen as a carrier gas, injector temperature set at 280 °C, injection volume of 2 μL, and the split mode of 10:1 according to a previously reported method (Russell & Rodriguez, 2023).

2.10. Quantitative Real-Time polymerase chain reaction (qRT-PCR) analysis

The total RNA from *C. reinhardtii* was extracted from *C. reinhardtii* using FreeZol Reagent R711 (Vazyme, China) and reverse-transcribed into cDNA using the SPARKscript II RT Plus kit (With gDNA Eraser) (Shandong Sparkjade Biotechnology Co., Ltd., China). The qRT-PCR analysis of selected genes related to CCM, i.e., carbonic anhydrase 1 (*CAH1*) (Zaidi et al., 2022), highlight activated 3 (*HLA3*) (Duanmu et al., 2009), and low carbon inducible A (*LCIA*) (Yamano et al., 2015), was performed using the SYBR Green qPCR Mix (with ROX) (Sparkjade, China) on a CFX Connect Real-Time PCR detection system (Bio-Rad, U.S.A.) with the primer sequences of *HLA3* (HLA3-F: GCTGGAGAAGACCTACG; HLA3-R: GCACGATGTTGTTGTAGAG), *LCIA* (LCIA-F: GCAGAAGAAGGCGAACAC; LCI1-R: GGTAGGCGATGATGTAGGT), *CAH1* (CAH1-F: GTTCCACTTCCACTCCAC; CAH1-R: TCAAGCAGCTCGTTATCG) (Benes & Castoldi, 2010). Transcription levels were calculated from the threshold cycle by interpolation of a standard curve. The 18S gene (18 s-F: ACCTGGTTGATCCTGCCAG; 18 s-R: TGATCCTTCCGCAGGTTCAC) was used as an internal standard for mRNA analysis.

2.11. Statistical analysis

Data are expressed as mean ± standard deviation. Statistical significance was evaluated by ANOVA and *t*-test using the SPSS program (Version 19.0, IBM SPSS, USA) at a level of $p < 0.05$.

3. Results and discussion

3.1. NH_4^+ tolerance of C. Reinhardtii

Photosynthetic organisms exhibit adaptability to varying nitrogen availability, environmental conditions, and nutrient provision, facilitating efficient utilization of inorganic nitrogen. This study evaluated the tolerance of *C. reinhardtii* to NH_4^+. Algal growth curves under different NH_4^+ concentrations showed a noticeable slowdown after 48 h compared to the standard TAP medium group. Furthermore, more significant inhibition of cell growth was observed under TAP + $1.0NH_4^+$ and TAP + 1.5 NH_4^+ conditions (Fig. 1A). Fig. 1B depicts the assimilation of NH_4^+ by *C. reinhardtii*, indicating a gradual decrease in NH_4^+ concentration across all groups during algal growth. The utilization rates in TAP + $0.5NH_4^+$, TAP + $0.7NH_4^+$, TAP + $1.0NH_4^+$, and TAP + $1.5NH_4^+$ were 64.0 %, 48.6 %, 25.3 %, and 18.6 %, respectively, and the NH_4^+ concentration in these four groups remained relatively constant after 72 h of culture, suggesting limited NH_4^+ utilization by algal cells, which is consistent with the findings shown in Fig. 1A. Previous studies have indicated that NH_4^+ absorption can lead to acidic environments and negatively affect microalgal growth (Zhou et al., 2022). As shown in Fig. 1C, after 24 h of cultivation, pH values exhibited a notable decrease to approximately pH 4.5–4.9 before stabilizing over time, suggesting that NH_4^+ absorption by *C. reinhardtii* produces a large number of H^+ ions mainly occurring during the initial stages of cultivation.

The effect of TAP medium with varying pH on the growth of *C. reinhardtii* cells was assessed (Fig. 1D). A significant decline in cell growth occurred when the pH fell below 6.5, confirming the adverse effects of pH on *C. reinhardtii* cell growth. Subsequently, four distinct experimental groups were established to investigate the effects of different concentrations of NH_4^+ while maintaining a consistent pH of 7 on algal cell growth (Fig. 1E). Growth observed in the trials involving TAP + $0.5NH_4^+$ and TAP + $0.7NH_4^+$ exhibited a slight increase com-

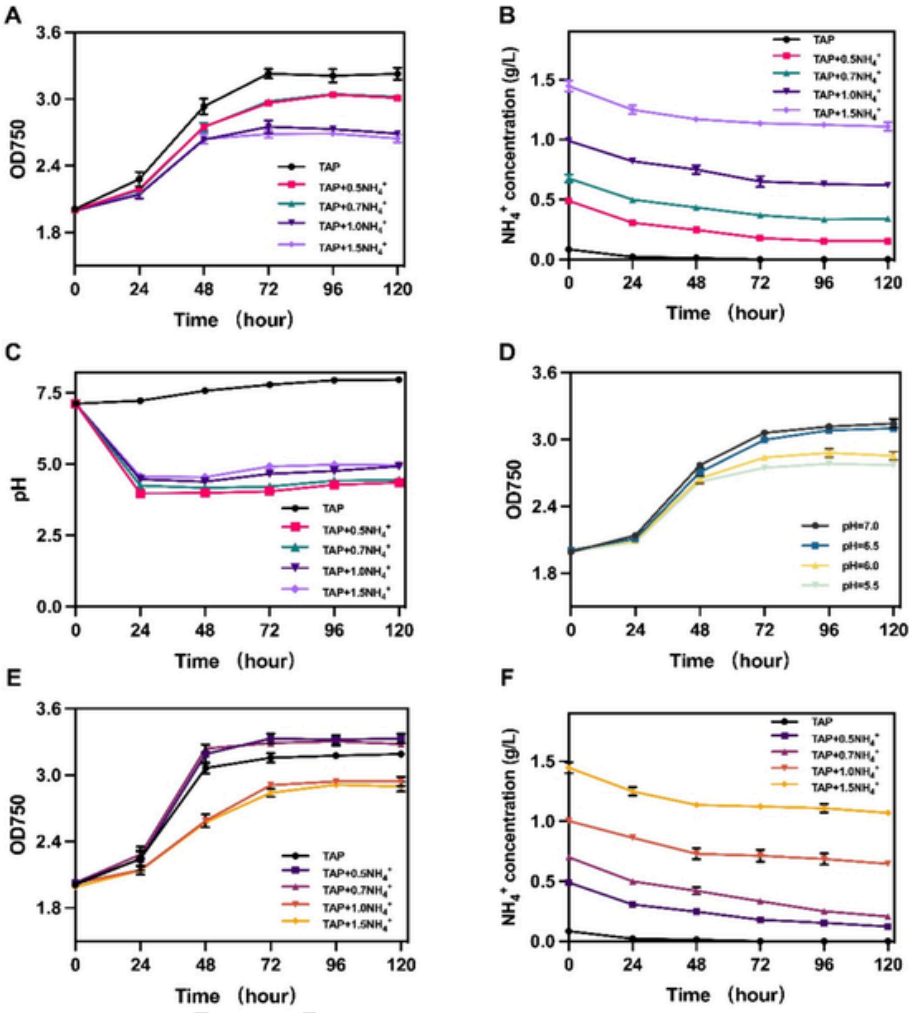

Fig. 1. The ammonium tolerance of *C. reinhardtii*. (A) The growth changes of algal cells in different ammonium concentration media, (B) The utilization of ammonium during cell growth, (C) Changes in solution pH, (D) The effect of different pH on cell growth, (E, F) The effect of different ammonium concentrations on cell growth and ammonium consumption when the pH is constant at 7. Data are shown as means ± standard error based on triplicate biological analysis(n = 3).

pared to the TAP trials, whereas trials with NH_4^+ concentrations of 1.0 and 1.5 g/L resulted in inhibited cell growth. NH_4^+ assimilation was monitored at a constant pH of 7 (Fig. 1F), revealed significantly higher utilization rates in the TAP + $0.5NH_4^+$ and TAP + $0.7NH_4^+$ trials (74.0 % and 54.2 %, respectively) than in the other two experimental groups (38.5 % in TAP + $1.0NH_4^+$ and 20.6 % in TAP + $1.5NH_4^+$). This finding suggested that cells exposed to higher NH_4^+ concentrations had lower viability than those exposed to lower concentrations.

Based on the aforementioned findings, when the NH_4^+ concentration was below 1.0 g/L, acidification of the medium emerged as the primary factor influencing cell growth, disrupting the ion-exchange balance between the original solution and the cell. This disruption affects electron transfer during photosynthesis, hampers cell metabolism, renders many enzymes inactive (Williams & Colman, 1996), and decreases the gross oxygen production in *C. reinhardtii* (Ihnken et al., 2014). Conversely, surplus NH_4^+ (exceeded 1.0 g/L) became a crucial limiting factor for algal cell growth. The substantial presence of NH_4^+ in the solution causes excess osmotic pressure, resulting in cellular dehydration and eventual cell death. Considering these findings, TAP medium with an additional 0.7 g/L NH_4^+ was chosen as the experimental NH_4^+ concentration to explore the potential of oyster shells to enhance *C. reinhardtii* growth in subsequent experiments.

3.2. Effects of powdered oyster shell on algae biomass production in high NH_4^+ medium

Zhou et al. previously demonstrated that the addition of $CaCO_3$, which is known for its low solubility that facilitates gradual dissolution into the acidic cultivation environment, can elevate pH levels and establish a stable growth environment for cells (Zhou et al., 2022). In this process, $CaCO_3$ effectively consumes H^+ to convert into CO_2 in acidic solution, and the resulting CO_2 can serve as a carbon source for cell growth. Oyster shells are recognized for their abundant $CaCO_3$ content (>95 %) (Miura et al., 1999), and their powder diameter may influence the availability of $CaCO_3$ and other essential nutrients (Xu et al., 2020). In this study, oyster shell powders of four different sizes (<0.15, 0.15 ~ 0.6, 0.6 ~ 1, and 1 ~ 2 mm) were utilized to investigate their efficacy in pH regulation and enhancement of algal cell growth, aiming for efficient biomass production.

3.2.1. Composition of oyster shells

The adult shells of the oyster *Crassostrea gigas* primarily consist of calcite ($CaCO_3$ accounts for 93.5 % of the composition), serving as an important carbon source. Additionally, oyster shells contain proteins, polysaccharides, and essential minerals crucial for microalgae growth, including magnesium (Mg), sodium (Na), copper (Cu), iron (Fe), nickel

(Ni) and strontium (Sr). The elemental composition of oyster shells was analyzed using ICP-MS, and the results are presented in Table 1. Notably, the phosphorus (P) content in oyster shells was relatively low, with a content of 0.1 %.

Table 1
The content of trace elements in oyster shell (n = 3 samples).

Element	Content (mg/kg)
Zn	25.5 ± 0.3
Fe	153.6 ± 1.2
Na	9688.2 ± 16.7
K	325.5 ± 6.2
Mg	1258.6 ± 15.4
Mn	82.8 ± 2.2
Cu	72.3 ± 1.1
Ni	24.1 ± 0.2

3.2.2. Cell growth, NH_4^+ consumption, pH value and Ca^{2+} concentration assessment

Algal cell growth was assessed on the basis of biomass accumulation (Fig. 2A). In the experimental setup, 0.7 g/L NH_4^+ was added to TAP medium. Fig. 2B illustrates that the peak NH_4^+ consumption rates for all experimental groups occurred within the initial 12 h, with an approximate usage of 0.32 g/L of NH_4^+. Despite substantial NH_4^+ uptake by algal cells, no discernible growth pattern was evident. This uptake led to acidification of the culture medium, causing the pH to swiftly decrease to approximately 3.8 after 12 h of cultivation (Fig. 2C).

Oyster shell powders of varying sizes were introduced at 12 h. Within the subsequent 12 h, the pH increased to a range of 5–7 depending on the particle size, and remained stable (pH = 7.05) after 36 h (Fig. 2C). It is noteworthy that, compared to oyster shell powders of other sizes, those with a diameter of < 0.15 mm exhibited a higher capacity to accumulate biomass, reaching up to 2.2 g/L after 60 h of cultivation (Fig. 2A). Subsequently, the NH_4^+ consumption rate notably decreased after 12 h of cultivation, and the maximum utilization of NH_4^+ was observed in the < 0.15 mm group at the end of cultivation, reach-

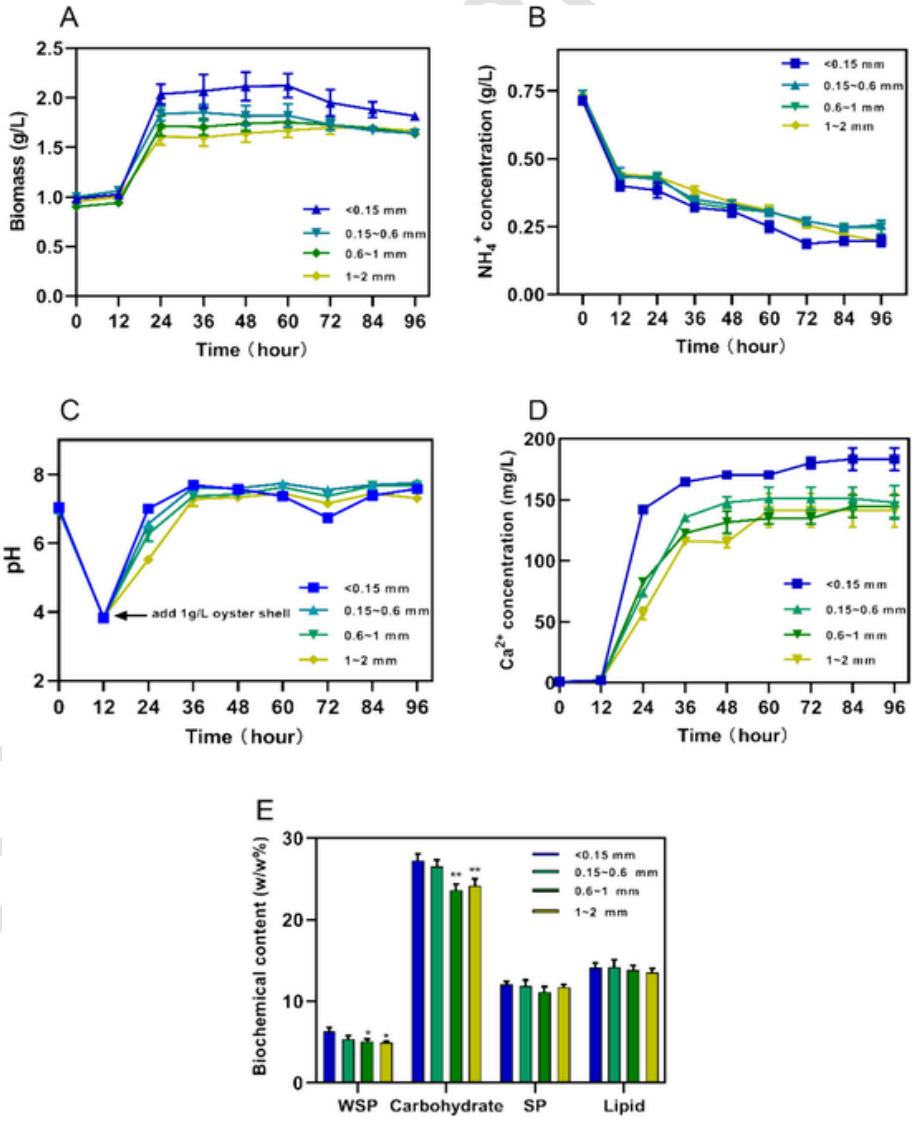

Fig. 2. Effect of oyster shell with different particle sizes on the growth of *C. reinhardtii* in the high ammonium medium. (A) Biomass, (B) Utilization of NH_4^+, (C) Solution pH, (D) Ca^{2+} content, (E) Biochemical contents. Data are shown as means ± standard error based on triplicate biological analysis (n = 3). The asterisk indicates statistical significance ($p < 0.05$).

ing 0.53 g L^{-1}, with a utilization rate of 70.6 % (Fig. 2B). The variation in the Ca^{2+} concentration over 96 h of cultivation is shown in Fig. 2D. A progressive, size-dependent increase in Ca^{2+} was observed with prolonged culture times. In particular, the hydrolytic capacity of oyster shell powders with particle size < 0.15 mm was notably higher than that of the other three groups, with the Ca^{2+} content in the solution reaching 189 mg L^{-1}.

These fluctuations in NH_4^+ consumption correspond to alterations in the pH and Ca^{2+} content of the solution, as mentioned earlier. When *C. reinhardtii* cells absorbed and utilized NH_4^+, they released a large amount of H^+, leading to a decrease in the pH of solution. Consequently, there was a gradual hydrolysis of $CaCO_3$ owing to the decrease in pH, resulting in a gradual increase in the Ca^{2+} content of the solution until the pH returned to neutral. These findings suggest that oyster shell powders with smaller particle sizes demonstrate superior hydrolytic ability, effectively buffering the pH of the solution, sustaining the normal growth of algal cells, and expediting nitrogen utilization. After 60 h of cultivation, a decrease in biomass was observed, which may be attributed to cells entering a stable period more rapidly during the second stage of growth. Therefore, cell aging and death are considered to be normal phenomena under these conditions.

3.2.3. Determination of biochemical components

At the end of the cultivation period, algal cells were harvested for biochemical analysis, as shown in Fig. 2E. Oyster shell powders ranging from 0.6 ~ 1 mm and 1 ~ 2 mm in size resulted in 0.8–1.2 % and 3.4–4.2 % significantly lower contents of water-soluble polysaccharides and total carbohydrates, respectively, than those of < 0.15 mm and 0.15 ~ 0.6 mm sizes ($P < 0.05$). This disparity may stem from oyster shell powders with larger particle sizes settling more rapidly, thereby hindering efficient utilization by algal cells in the system. Changes in protein and lipid contents were not significant across oyster shell powders of different sizes ($P > 0.05$). These findings highlight the influence of oyster shell size on specific biochemical components, particularly water-soluble polysaccharides and total carbohydrates.

Smaller oyster shell powders exhibit a notable pH-buffering capacity, promote cell growth, and facilitate the accumulation of intracellular products. Trace elements such as zinc, iron, and manganese are essential for the growth of planktonic algae (Sahu et al., 2019). The decomposition of powdered oyster shell results in the production of organic matter and trace elements, which are subsequently absorbed by algal cells. Moreover, acid hydrolysis of powdered oyster shell generates compounds such as CO_3^{2-} and HCO_3^-, serving as inorganic carbon sources for cellular development. These findings emphasize the multifaceted roles of powdered oyster shell in enhancing algal proliferation and their possible utilization in various biotechnological applications.

3.3. The synergistic effect of carbon and nitrogen sources on algae growth

To further elucidate the synergistic impact of nitrogen and carbon in the aforementioned system, three experimental groups were established to analyze algal cell growth: TAP, NaOH-0.7NH_4^+, and oyster shell-0.7NH_4^+. The objective was to clarify the enhancing effect of NH_4^+ on cell growth and validate the carbon supply capacity of oyster shells. The pH was maintained at 7.5 using a pH automatic titrator in the NaOH-0.7NH_4^+ group, while oyster shell powders with particle sizes of < 0.15 mm were added at a dose of 1 g/L in the oyster shell-0.7NH_4^+ group.

3.3.1. Evaluating the carbon-supplying capacity and NH_4^+ utilization enhancement of powdered oyster shell

As shown in Fig. 3A, microalgae cultivated in the oyster shell-0.7 NH_4^+ and NaOH-0.7NH_4^+ media reached the maximum biomass levels of 2.36 and 2.22 g/L, respectively, surpassing those of the TAP group by 0.44 (22.9 %) and 0.3 (15.6 %) ($P < 0.05$), after 48 h of cultivation. The changes in NH_4^+ concentration (Fig. 3B) revealed that NH_4^+ was

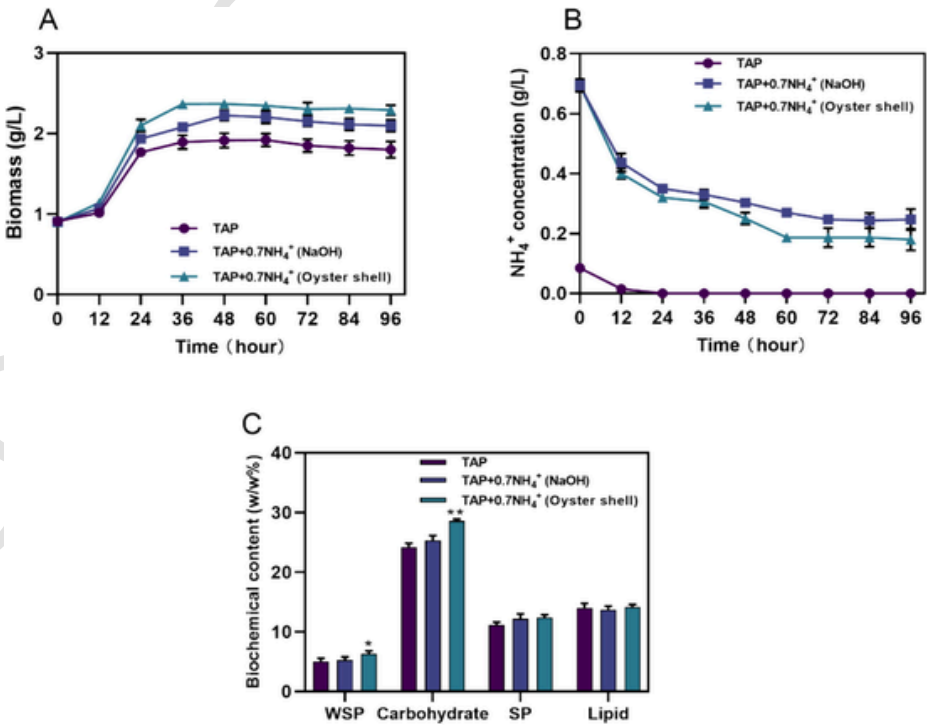

Fig. 3. Evaluation of algal growth on TAP (control) and TAP containing NaOH-0.7NH_4^+ (high nitrogen source) and oyster shell-0.7NH_4^+ (high nitrogen and carbon source). (A) Biomass, (B) Utilization of NH_4^+, (C) Biochemical contents. Data are shown as means ± standard error based on triplicate biological analysis (n = 3). The asterisk indicates statistical significance ($p < 0.05$).

depleted after 12 h of cultivation in the TAP group, whereas NH_4^+ remained abundantly available to algal cells in the other two groups with supplemental nitrogen sources, resulting in continued biomass accumulation until reaching a growth plateau. Throughout the cultivation period, up to 0.55 g/L of NH_4^+ was consumed by algal cells, with a utilization rate of 76.3 %. In both experimental sets, the pH of the solution remained constant, facilitating the absorption and utilization of a significant nitrogen source by the cells. An adequate nitrogen supply plays a dual role: sustaining chlorophyll synthesis, thus boosting photosynthetic efficiency, and promoting the seamless biosynthesis of amino acids, nucleic acids, proteins, and other key biomolecules, consequently fostering the growth of algal cells. The increased biomass accumulation in the oyster shell-0.7 NH_4^+ group is attributed to the abundant inorganic carbon (CO_3^{2-}, HCO_3^-, and CO_2) generated through the hydrolysis of oyster shells. Inorganic carbon enhances the photosynthetic efficiency of algal cells by boosting their assimilation of inorganic carbon and modulating the pathways involved in organic substance synthesis. Moreover, the uptake of inorganic carbon triggers the CCM, facilitating the optimal allocation of inorganic carbon within the cell.

As shown in Fig. 3C, analysis of intracellular components at the cultivation period's end revealed higher accumulation of polysaccharides (6.3 %) and carbohydrates (27.5 %) in the oyster shell-0.7NH_4^+ group, demonstrating the synergistic effects of nitrogen and carbon on biomass accumulation in algal cells. Compared to the TAP group, the protein content in the shell-0.7NH_4^+ group showed a slight increase (from 11.2 % to 12.4 %), while lipid accumulation was slightly decreased (from 14.5 % to 13.9 %). These findings suggest that excessive supplementation of nitrogen sources enhanced the accumulation of proteins while concurrently reducing lipid accumulation. Previous studies have indicated that during acclimation to nitrogen deprivation, *C. reinhardtii* cells accumulate significant quantities of starch and form lipid bodies (Work et al., 2010). The presence of powdered oyster shell further enhanced these trends, indicating a complex interplay between nitrogen availability, carbon sources, and the composition of intracellular components in *C. reinhardtii*.

Table 2
The fatty acid content of the different processing groups (n = 3 samples).

	Different processing groups		
	TAP	TAP-0.7NH_4^+ (NaOH)	TAP-0.7NH_4^+ (Oyster shell)
Fatty acids	Fatty acid content (μg g^{-1})		
C16:0	4.97 ± 0.12	7.13 ± 0.11	7.23 ± 0.14
C16:1	0.039 ± 0.002	0.041 ± 0.003	0.052 ± 0.002
C18:0	0.37 ± 0.09	0.73 ± 0.12	0.72 ± 0.14
C18:1n9c	1.69 ± 0.08	2.93 ± 0.07	3.00 ± 0.06
C18:2n6c	1.58 ± 0.09	2.88 ± 0.07	3.72 ± 0.02
C18:3n3	4.68 ± 0.15	6.50 ± 0.11	6.90 ± 0.12
C20:0	0.017 ± 0.003	0.025 ± 0.001	0.030 ± 0.004
C20:2	0.01 ± 0.003	0.011 ± 0.002	0.014 ± 0.005
C22:0	0.024 ± 0.002	0.027 ± 0.001	0.033 ± 0.001
C22:1n9c	0.01 ± 0.002	0.017 ± 0.002	0.016 ± 0.001
C24:0	0.023 ± 0.001	0.029 ± 0.003	0.028 ± 0.004

3.3.2. Fatty acid composition analysis

A nitrogen-rich culture medium promotes algal cell growth while constraining oil accumulation and modifying fatty acid composition (Ferrel Ballestas et al., 2023; Liufu et al., 2023). Typically, synthesized fatty acids have chain lengths ranging from C16 to C18 (Liu et al., 2021). The results of the fatty acid analysis are shown in Table 2. In *C. reinhardtii*, 35 FAMEs were detected using mixed standards, consistent with previous studies, indicating significant alterations in long-chain fatty acids, such as palmitic acid (C16), stearic acid (C18), arachidic acid (C20), behenic acid (C22), and tetracosanoic acid (C24). Monounsaturated fatty acids (MUFAs), such as palmitelaidic acid (C16:1), oleic acid (C18:1n9c), and erucic acid (C22:1n9c), as well as polyunsaturated fatty acids (PUFAs), such as linoleic acid (C18:2n6c), linolenic acid (C18:3n3), and arachidonic acid (C20:2), displayed notable variations. Specifically, the contents of C16, C18, C18:1n-9c, C18:2n-6c, and C18:3n-3 increased under high NH_4^+ conditions compared to the TAP medium. The total unsaturated fatty acid content in NaOH-0.7NH_4^+ and oyster shell-0.7NH_4^+ groups increased by 51.5 % and 62.1 % compared to the TAP group. Algal cells exhibited increased lipid accumulation under nitrogen-deprived conditions, whereas a nitrogen-rich medium led to a relative reduction in lipid accumulation.

3.3.3. DIC levels variation and HLA3, LCIA, and CAH1 mRNA relative expression in the CCMs

It has been proposed that CCM utilizing HCO_3^- uptake is the most prevalent strategy for DIC utilization by macroalgae (Raven & Beardall, 2014). To validate the utilization of powdered oyster shell as an inorganic carbon source for algal cell growth, DIC analysis of the medium was conducted at various time intervals (0, 6, 12, 15, and 18 h). In this study, TAP, NaOH-0.7NH_4^+, and oyster shell-0.7NH_4^+ groups were examined. Fig. 4A shows that the DIC content sharply increased in all three groups at 6 h due to aeration following the change of culture medium, resulting in the dissolution of atmospheric CO_2 into the medium and a subsequent rapid rise in DIC content. Analysis of the changes in DIC content in the NaOH-0.7NH_4^+ and oyster shell-0.7NH_4^+ groups revealed that the oyster shell-0.7NH_4^+ group exhibited a significantly higher inorganic carbon content (6.98 × 10^3 μmol L^{-1}) than the NaOH group (4.76 × 10^3 μmol L^{-1}) at 6 h. This disparity could be attributed to algal cells absorbing NH_4^+, causing a decrease in solution pH, thereby promoting the hydrolysis of oyster shells and consequent generation of a large amount of inorganic carbon. After 12 h,

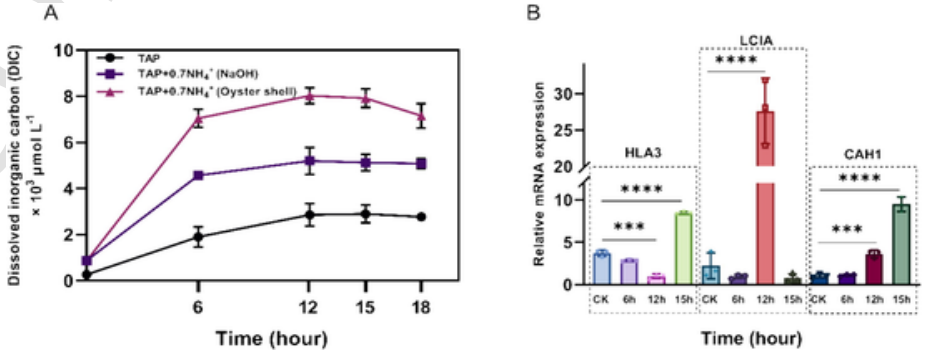

Fig. 4. (A) Variations in the dissolution of inorganic carbon were observed at various time intervals; (B) The transcript levels of *HLA3*, *LCIA*, and *CAH1* at different time points were determined by real-time qPCR. And calculated from Ct values using the $2^{-\Delta\Delta t}$ method after all results were normalized against the 18S housekeeping gene. Data are shown as means ± standard error based on triplicate biological analysis(n = 3). The asterisk indicates statistical significance ($p < 0.05$).

the oyster shell-0.7NH_4^+ group reached the highest inorganic carbon content, at 8.02 × 10^3 μmol L^{-1}. Subsequently, a decline in inorganic carbon content was observed in this group from 15 to 18 h, indicating the utilization of inorganic carbon by algal cells.

According to the CCM model of *C. reinhardtii*, atmospheric CO_2 is initially converted into HCO_3^-, which is then transported from the extracellular environment into the cystic-like cavity through a series of transport proteins, including plasma membrane *HLA* and chloroplast membrane *LCI*. Subsequently, the accumulated HCO_3^- is dehydrated into CO_2 by the *CA*, thus increasing the local concentration of CO_2 around RuBisCO, which enhances photosynthesis and promotes cell growth (Gao et al., 2015; Kono & Spalding, 2020). To investigate the impact of inorganic carbon generation on the CCM, oyster shell-0.7NH_4^+ was used as the experimental group, followed by sampling at various time intervals (0, 6, 12, and 15 h) and analysis of the relative expression of *HLA3*, *LCIA*, *and CAH1* through qRT-PCR.

The expression of the three genes decreased at the 6 h mark, which could be attributed to the release of a substantial amount of H^+ when cells absorb NH_4^+, leading to a pH decrease in the solution that impacts cell growth and metabolism deceleration (Wang et al., 2019). The progression of this phenomenon slowed down between the 6th and 12th h due to oyster shell hydrolysis, resulting in elevated levels of CO_3^{2-} and HCO_3^- in the solution. Currently, an increased amount of inorganic carbon is transported into the cell through active mechanisms, leading to a decrease in the expression of *HLA3*. The expression level of *HLA3* exhibited an 8-fold increase at 15 h compared to 12 h. This phenomenon could be attributed to rapid cell growth during this phase, a reduction in the inorganic carbon content within the solution, and the activation of *HLA3* to facilitate the translocation of extracellular inorganic carbon (Fig. 4B), which was consistent with findings in a previous study (Gao et al., 2015). Moreover, the chloroplast membrane *LCIA* transporter protein transports a large amount of intracellular inorganic carbon to the thylakoid cavity, ensuring the progress of photosynthesis. Consequently, its expression level increased sharply at 12 h, reaching approximately 27-fold higher than that at 6 h (Fig. 4B). This process was also accompanied by the catalytic action of *CAH1* (HCO_3^- dehydration to CO_2), resulting in a 5-fold increase in activity of *CAH1* at 12 h compared to 6 h; achieving enhanced levels of articulation within a span of 15 h (Fig. 4B). The activation of downstream genes enhances the utilization of HCO_3^-, thereby preventing excessive HCO_3^- accumulation during the transportation process and ultimately leading to the normalization of *LCIA* expression at 15 h. Several studies have shown that *LCIA* is linked to the uptake of HCO_3^- under low-carbon conditions (Yamano et al., 2015). This change in gene expression also demonstrated that the rapid growth of cells was not only due to the restoration of the solution environment to neutrality, but more importantly, that the decomposition of $CaCO_3$ provides an additional inorganic carbon source for cell growth.

3.4. Effect of oyster shells on algal cell flocculation

Positively charged metal ions, such as Fe^{2+}, Al^{3+}, Ca^{2+}, and Mg^{2+}, have been extensively studied for their ability to induce flocculation (Kwon et al., 2011; Wyatt et al., 2012). In this culture system, shellfish shells rich in Ca^{2+} hold potential as a means of algae removal and the elimination of eutrophic substances through coagulation and precipitation methods. In such scenarios, the Ca^{2+} ion can induce flocculation of algae by forming ionic bonds with CO_2 or CO_3^{2-} on their surface, or by precipitating with PO_4^{3-} or NO_3^- ions to create various ionic compounds in the solution (Nam et al., 2017). As a preliminary test, the algae solution was poured into a 500 mL beaker at the end of the cultivation, resulting settling efficiency of 61.7 % after 3 h of settling, higher 19.2 % than TAP group (Fig. 5A). Additionally, the zeta potential of *C. reinhardtii* in the oyster shell-0.7NH_4^+ group was − 21.2 mV, causing 42.1 % reduced from TAP group (Fig. 5A), indicating a significantly higher tendency for aggregation compared to the other two groups (Fig. 5B). The significant settlement observed could be attributed to the presence of a large amount of Ca^{2+} in the solution.

Subsequently, to elucidate the impact of Ca^{2+} on the flocculation efficiency of algal cells, various concentration gradients were established using calcium chloride ($CaCl_2$), followed by the evaluation of different algal biomass solutions. Ca^{2+} exhibited efficiencies exceeding 80 % at the two highest cell concentrations tested. At biomass of 2.4 g L^{-1}, the maximum flocculation efficiency reached 67.6 % when the Ca^{2+} concentration in the solution was 200 mg L^{-1}, representing a 27.7 % increase compared to the starting point with no added Ca^{2+} (Fig. 5C). In prior experiments, the concentration of Ca^{2+} generated through the hydrolysis of powdered oyster shell in solution approached 190 mg L^{-1} (Fig. 2B), leading to enhanced sedimentation effectiveness attributed to cellular flocculation. A plausible explanation was that an excessive amount of flocculant surpassing the optimal level could generate an excess of positive charges, thereby stabilizing the suspended cell particles through charge repulsion and steric hindrance. Conversely, higher algal cell concentrations require more Ca^{2+} to promote flocculation. In industrial production processes, microalgae cultivation is predominantly conducted in open raceway ponds. For large-scale harvesting, chemical flocculants are commonly utilized, but their residues can cause contamination in subsequent microalgae cultivation processes. From an environmental and sustainable perspective, oyster shell powders are nontoxic, noncorrosive, and easy-to-handle, making them a promising alternative to chemical flocculants in high NH_4^+ environments.

4. Conclusions

This study evaluated the effects of powdered oyster shell on microalgae growth and harvesting in high NH_4^+ medium. Powdered oyster shell effectively functioned as a liming agent and supplemental carbon source for microalgae growth, achieving a biomass production of up to 2.36 g/L in high NH_4^+ medium. Furthermore, powdered oyster shell also served as a bio-flocculant, promoting the aggregation of microalgae for biomass harvesting. In conclusion, this research presents a promising strategy to enhance biomass production and cost-effective harvesting of microalgae in high NH_4^+ medium by leveraging powdered oyster shell as a liming agent, supplement carbon source, and bioflocculant.

CRediT authorship contribution statement

Jikang Sui: Writing – review & editing, Writing – original draft, Validation, Methodology, Investigation, Formal analysis, Data curation, Conceptualization. **Yuxuan Cui:** Methodology, Investigation, Formal analysis. **Jinku Zhang:** Methodology, Investigation, Formal analysis. **Shiyang Li:** Methodology, Investigation, Formal analysis. **Yue Zhao:** Methodology, Investigation, Formal analysis. **Mingkai Bai:** Methodology, Investigation, Formal analysis. **Guangxin Feng:** Writing – review & editing, Visualization, Validation, Methodology, Formal analysis. **Haohao Wu:** Writing – review & editing, Supervision, Resources, Project administration, Funding acquisition.

Declaration of competing interest

The authors declare that they have no known competing financial interests or personal relationships that could have appeared to influence the work reported in this paper.

Data availability

The data that has been used is confidential.

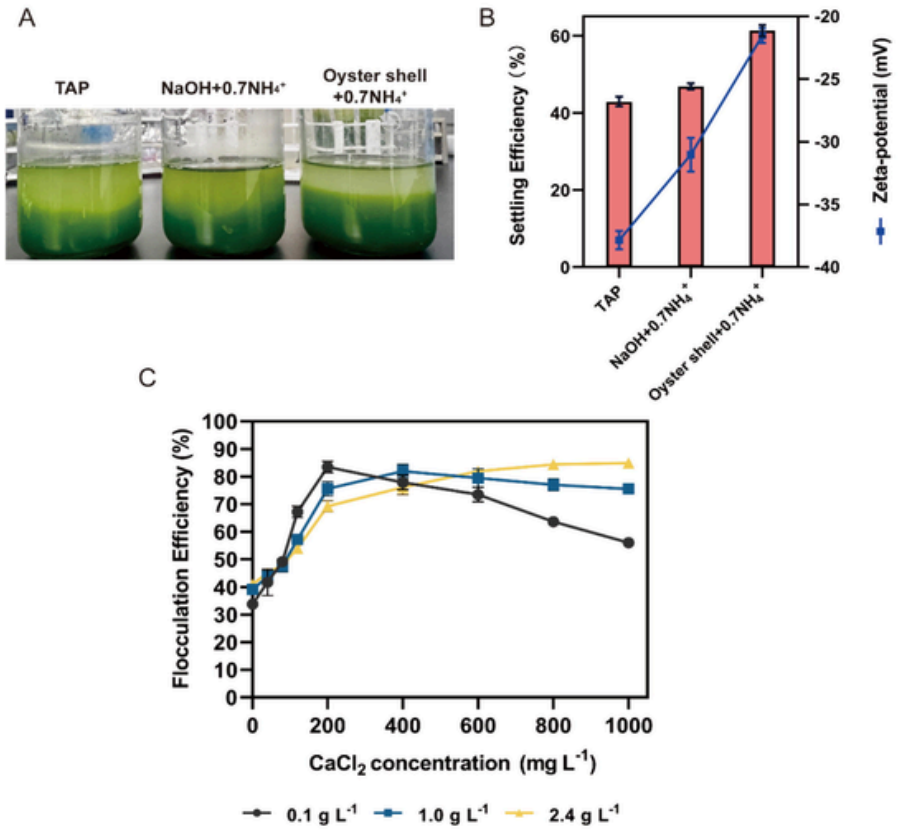

Fig. 5. (A) The settling effect of the solution after standing for 3 h. (B) Effect of consecutive treatment with oyster shells on settling efficiency and zeta-potential value. (C) and (D) Flocculation efficiencies of $CaCl_2$ at three cell concentrations of C. reinhardtii. Data are shown as means ± standard error based on triplicate biological analysis(n = 3). There is no statistical significance.

Acknowledgements

This work was financially supported by National Natural Science Foundation of China (No. 32272240), Postdoctoral Fellowship Program of CPSF (No. GZC20232506), and Shandong Postdoctoral Science Foundation (No. SDBX202302012). The authors thank Shanghai Bioprofile Biotechnology Co., Ltd for technical assistance in mass spectroscopy.

Appendix A. Supplementary data

Supplementary data to this article can be found online at https://doi.org/10.1016/j.biortech.2024.130904.

References

Bai, D., Jia, M., Zhao, X., Ban, R., Shen, F., Li, X., Xu, S., 2003. L(+)-lactic acid production by pellet-form Rhizopus oryzae R1021 in a stirred tank fermentor. Chem. Eng. Sci. 58 (3), 785–791. https://doi.org/10.1016/S0009-2509(02)00608-5.

Banerjee, S., Ray, A., Das, D., 2021. Optimization of *Chlamydomonas reinhardtii* cultivation with simultaneous CO_2 sequestration and biofuels production in a biorefinery framework. Sci. Total Environ. 762, 143080. https://doi.org/10.1016/j.scitotenv.2020.143080.

Benes, V., Castoldi, M., 2010. Expression profiling of microRNA using real-time quantitative PCR, how to use it and what is available. Methods 50 (4), 244–249. https://doi.org/10.1016/j.ymeth.2010.01.026.

Collos, Y., Harrison, P.J., 2014. Acclimation and toxicity of high ammonium concentrations to unicellular algae. Mar Pollut Bull 80 (1–2), 8–23. https://doi.org/10.1016/j.marpolbul.2014.01.006.

Darwish, R., Gedi, M.A., Akepach, P., Assaye, H., Zaky, A.S., Gray, D.A., 2020. *Chlamydomonas reinhardtii* Is a Potential Food Supplement with the Capacity to Outperform *Chlorella* and *Spirulina*. Appl. Sci. 10 (19), 6736. https://doi.org/10.3390/app10196736.

Duanmu, D., Miller, A.R., Horken, K.M., Weeks, D.P., Spalding, M.H., 2009. Knockdown of limiting-CO_2–induced gene HLA3 decreases HCO_3^- transport and photosynthetic Ci affinity in *Chlamydomonas reinhardtii*. Proc. Natl. Acad. Sci. 106 (14), 5990–5995. https://doi.org/10.1073/pnas.0812885106.

Ermilova EV, Z.Z., Nikitin MM, Lapina TV, Fernández E. 2010. Regulation by light of ammonium transport systems in *Chlamydomonas reinhardtii*. *Plant, Cell & Environment* **33**(6), 1049-1056. https://doi.org/10.1111/j.1365-3040.2010.02126.x

Ferrel Ballestas, F.R., Titica, M., Legrand, J., Pilon, L., Cogne, G., 2023. Prediction of the radiation characteristics and the light absorption rate of *Chlamydomonas reinhardtii* cultivated under a progressive nitrogen starvation and accumulating carbon reserves. J. Quant. Spectrosc. Radiat. Transf. 309, 108708. https://doi.org/10.1016/j.jqsrt.2023.108708.

Fukuzawa, H., Miura, K., Ishizaki, K., Kucho, K.-I., Saito, T., Kohinata, T., Ohyama, K., 2001. Ccm1, a regulatory gene controlling the induction of a carbon-concentrating mechanism in *Chlamydomonas reinhardtii* by sensing CO_2 availability. Proc. Natl. Acad. Sci. 98 (9), 5347–5352. https://doi.org/10.1073/pnas.081593498.

Gao, H., Wang, Y., Fei, X., Wright, D.A., Spalding, M.H., 2015. Expression activation and functional analysis of HLA3, a putative inorganic carbon transporter in *Chlamydomonas reinhardtii*. Plant J. 82 (1), 1–11. https://doi.org/10.1111/tpj.12788.

Giordano, M., Beardall, J., Raven, J.A., 2005. CO2 concentrating mechanisms in algae: mechanisms, environmental modulation, and evolution. Annu Rev Plant Biol 56, 99–131. https://doi.org/10.1146/annurev.arplant.56.032604.144052.

Gorman, D.S., Levine, R.P., 1965. Cytochrome f and plastocyanin: their sequence in the photosynthetic electron transport chain of *Chlamydomonas reinhardi*. Proc. Natl. Acad. Sci. 54 (6), 1665–1669. https://doi.org/10.1073/pnas.54.6.1665.

He, Y., Chen, L., Zhou, Y., Chen, H., Zhou, X., Cai, F., Huang, J., Wang, M., Chen, B., Guo, Z., 2016. Analysis and model delineation of marine microalgae growth and lipid accumulation in flat-plate photobioreactor. Biochem. Eng. J. 111, 108–116. https://doi.org/10.1016/j.bej.2016.03.014.

Hurd, C.L., Hepburn, C.D., Currie, K.I., Raven, J.A., Hunter, K.A., 2009. Testing the effects of ocean acidification on algal metabolism: Considerations for experimental designs. J. Phycol. 45 (6), 1236–1251. https://doi.org/10.1111/j.1529-8817.2009.00768.x.

Ihnken, S., Beardall, J., Kromkamp, J.C., Gómez Serrano, C., Torres, M.A., Masojídek, J., Malpartida, I., Abdala, R., Jerez, C.G., Malapascua, J.R., Navarro, E., Rico, R.M., Peralta, E., Ezequil, J.P.F., Figueroa, F.L., 2014. Light acclimation and pH perturbations affect photosynthetic performance in Chlorella mass culture. Aquat. Biol. 22, 95–110. https://doi.org/10.3354/ab00586.

Kono, A., Spalding, M.H., 2020. LCI1, a *Chlamydomonas reinhardtii* plasma membrane

protein, functions in active CO_2 uptake under low CO_2. Plant J. 102 (6), 1127–1141. https://doi.org/10.1111/tpj.14761.
Kwon, D., Jung, C., Park, K., Lee, C.G., Lee, J., 2011. Flocculation Characteristics of Microalgae Using Chemical Flocculants. Korean Society for Biotechnology and Bioengineering Journal 26 (2), 143–150. https://doi.org/10.7841/ksbbj.2011.26.2.143.
Liu, Y.X., Yang, T.O., Yuan, D.X., Wu, X.Y., 2010. Study of municipal wastewater treatment with oyster shell as biological aerated filter medium. Desalination 254 (1–3), 149–153. https://doi.org/10.1016/j.desal.2009.12.003.
Liu, J., Yin, J., Ge, Y., Han, H., Liu, M., Gao, F., 2021. Improved lipid productivity of Scenedesmus obliquus with high nutrient removal efficiency by mixotrophic cultivation in actual municipal wastewater. Chemosphere 285, 131475. https://doi.org/10.1016/j.chemosphere.2021.131475.
Liufu, W., Di, M., Yingying, P., Liqiu, S., Wenzhi, W., 2023. Nitrogen limitation and hydrogen peroxide act synergistically to enhance lipids accumulation via ROS/Ca^{2+} dependent mechanism in *Chlorella sorokiniana*. Algal Res. 70, 102974. https://doi.org/10.1016/j.algal.2023.102974.
Markou, G., Muylaert, K., 2016. Effect of light intensity on the degree of ammonia toxicity on PSII activity of *Arthrospira platensis* and *Chlorella vulgaris*. Bioresour. Technol. 216, 453–461. https://doi.org/10.1016/j.biortech.2016.05.094.
Miura, T., Takayama, Y., Nakano, M., 1999. Effect of Shellfish Calcium on the Apparent Absorption of Calcium and Bone Metabolism in Ovariectomized Rats. Biosci. Biotech. Bioch. 63 (1), 40–45. https://doi.org/10.1271/bbb.63.40.
Mondal, M., Ghosh, A., Oinam, G., Tiwari, O.N., Gayen, K., Halder, G.N., 2017. Biochemical responses to bicarbonate supplementation on biomass and lipid productivity of Chlorella Sp. BTA9031 isolated from Coalmine area. Environ. Prog. Sustain. Energy 36 (5), 1498–1506. https://doi.org/10.1002/ep.12594.
Moon, M., Kim, C.W., Park, W.-K., Yoo, G., Choi, Y.-E., Yang, J.-W., 2013. Mixotrophic growth with acetate or volatile fatty acids maximizes growth and lipid production in *Chlamydomonas reinhardtii*. Algal Res. 2 (4), 352–357. https://doi.org/10.1016/j.algal.2013.09.003.
Morris, J.P., Backeljau, T., Chapelle, G., 2019. Shells from aquaculture: a valuable biomaterial, not a nuisance waste product. Rev. Aquac. 11 (1), 42–57. https://doi.org/10.1111/raq.12225.
Nam, G., Choi, Y.-H., Lee, N., Ahn, J.W., 2017. Effect by Alkaline Flocculation of Algae and Phosphorous from Water Using a Calcined Waste Oyster Shell. Water 9 (9), 661. https://doi.org/10.3390/w9090661.
Pandey, A., Pathak, V.V., Kothari, R., Black, P.N., Tyagi, V.V., 2019. Experimental studies on zeta potential of flocculants for harvesting of algae. J. Environ. Manage. 231, 562–569. https://doi.org/10.1016/j.jenvman.2018.09.096.
Raven, J.A., Beardall, J., 2014. CO2 concentrating mechanisms and environmental change. Aquat. Bot. 118, 24–37. https://doi.org/10.1016/j.aquabot.2014.05.008.
Russell, C., Rodriguez, C., 2023. Lipid extraction from *Chlorella vulgaris* & *Haematococcus pluvialis* using the switchable solvent DMCHA for biofuel production. Energy 278, 127983. https://doi.org/10.1016/j.energy.2023.127983.
Sahu, Y.K., Patel, K.S., Martín-Ramos, P., Rudzińska, M., Górnaś, P., Towett, E.K., Martín-Gil, J., Tarkowska-Kukuryk, M., 2019. Algal characterization and bioaccumulation of trace elements from polluted water. Environ. Monit. Assess. 192 (1), 38. https://doi.org/10.1007/s10661-019-8001-3.
Shitanaka, T., Fujioka, H., Khan, M., Kaur, M., Du, Z.-Y., Khanal, S.K., 2024. Recent advances in microalgal production, harvesting, prediction, optimization, and control strategies. Bioresour. Technol. 391, 129924. https://doi.org/10.1016/j.biortech.2023.129924.
Su, Y., 2021. Revisiting carbon, nitrogen, and phosphorus metabolisms in microalgae for wastewater treatment. Sci. Total Environ. 762, 144590. https://doi.org/10.1016/j.scitotenv.2020.144590.
Surendra, K.C., Angelidaki, I., Khanal, S.K., 2022. Bioconversion of waste-to-resources (BWR-2021): Valorization of industrial and agro-wastes to fuel, feed, fertilizer, and biobased products. Bioresour. Technol. 347, 126739. https://doi.org/10.1016/j.biortech.2022.126739.
Trivedi, J., Agrawal, D., Atray, N., Ray, A., 2022. Enhanced lipid production in Scenedesmus obliquus via nitrogen starvation in a two-stage cultivation process and evaluation for biodiesel production. Fuel 316, 123418. https://doi.org/10.1016/j.fuel.2022.123418.
Wang, J., Zhou, W., Chen, H., Zhan, J., He, C., Wang, Q., 2019. Ammonium Nitrogen Tolerant Chlorella Strain Screening and Its Damaging Effects on Photosynthesis. Front. Microbiol. 9, 912924. https://doi.org/10.3389/fmicb.2018.03250.
Williams, T.G., Colman, B., 1996. The effects of pH and dissolved inorganic carbon on external carbonic anhydrase activity in Chlorella saccharophila. Plant Cell Environ. 19 (4), 485–489. https://doi.org/10.1111/j.1365-3040.1996.tb00341.x.
Work, V.H., Radakovits, R., Jinkerson, R.E., Meuser, J.E., Elliott, L.G., Vinyard, D.J., Laurens, L.M., Dismukes, G.C., Posewitz, M.C., 2010. Increased lipid accumulation in the Chlamydomonas reinhardtii sta7-10 starchless isoamylase mutant and increased carbohydrate synthesis in complemented strains. Eukaryot Cell 9 (8), 1251–1261. https://doi.org/10.1128/ec.00075-10.
Wyatt, N.B., Gloe, L.M., Brady, P.V., Hewson, J.C., Grillet, A.M., Hankins, M.G., Pohl, P.I., 2012. Critical conditions for ferric chloride-induced flocculation of freshwater algae. Biotechnol. Bioeng. 109 (2), 493–501. https://doi.org/10.1002/bit.23319.
Xu, Y., Ye, J., Zhou, D., Su, L., 2020. Research progress on applications of calcium derived from marine organisms. Sci. Rep. 10 (1), 18425. https://doi.org/10.1038/s41598-020-75575-8.
Yamano, T., Sato, E., Iguchi, H., Fukuda, Y., Fukuzawa, H., 2015. Characterization of cooperative bicarbonate uptake into chloroplast stroma in the green alga *Chlamydomonas reinhardtii*. PNAS 112 (23), 7315–7320. https://doi.org/10.1073/pnas.1501659112.
Ye, Y., Ngo, H.H., Guo, W., Liu, Y., Chang, S.W., Nguyen, D.D., Liang, H., Wang, J., 2018. A critical review on ammonium recovery from wastewater for sustainable wastewater management. Bioresour. Technol. 268, 749–758. https://doi.org/10.1016/j.biortech.2018.07.111.
Zaidi, S., Srivastava, N., Kumar Khare, S., 2022. Microbial carbonic anhydrase mediated carbon capture, sequestration & utilization: A sustainable approach to delivering bio-renewables. Bioresour. Technol. 365, 128174. https://doi.org/10.1016/j.biortech.2022.128174.
Zhang, Z., Hu, Y.-B., 2023. Assessment on seasonal acidification and its controls in the Muping Marine Ranch, Yantai. China. Marine Pollution Bulletin 189, 114826. https://doi.org/10.1016/j.marpolbul.2023.114826.
Zhao, Y., Shi, R., Bian, X., Zhou, C., Zhao, Y., Zhang, S., Wu, F., Waterhouse, G.I.N., Wu, L.-Z., Tung, C.-H., Zhang, T., 2019. Ammonia Detection Methods in Photocatalytic and Electrocatalytic Experiments: How to Improve the Reliability of NH3 Production Rates? Adv. Sci. 6 (8), 1802109. https://doi.org/10.1002/advs.201802109.
Zhou, Y., He, Y., Xiao, X., Liang, Z., Dai, J., Wang, M., Chen, B., 2022. A novel and efficient strategy mediated with calcium carbonate-rich sources to remove ammonium sulfate from rare earth wastewater by heterotrophic Chlorella species. Bioresour. Technol. 343, 125994. https://doi.org/10.1016/j.biortech.2021.125994.